BULLETIN OF BIOMATHEMATICS

Bulletin of Biomathematics, 2024, 2(2), 198–217

https://www.bulletinbiomath.org
ISSN Online: 2980-1869 / Open Access
https://doi.org/10.59292/bulletinbiomath.2024009

RESEARCH PAPER

The effect of amyloid beta, membrane, and ER pathways on the fractional behavior of neuronal calcium

Brajesh Kumar Jha [1,*,‡], **Vora Hardagna Vatsal** [1,‡] **and Tajinder Pal Singh** [1,‡]

[1]Department of Mathematics, School of Technology, Pandit Deendayal Energy University, Gandhinagar, 382426 Gujarat, India

* Corresponding Author
‡ brajeshjha2881@gmail.com (Brajesh Kumar Jha); hardagna.vora@gmail.com (Vora Hardagna Vatsal); Tajinder.Singh@spt.pdpu.ac.in (Tajinder Pal Singh)

Abstract

Calcium signal transduction is essential for cellular activities such as gene transcription, death, and neuronal plasticity. Dynamical changes in the concentration of calcium have a profound effect on the intracellular activity of neurons. The Caputo fractional reaction-diffusion equation is a useful tool for modeling the intricate biological process involved in calcium concentration regulation. We include the Amyloid Beta, STIM-Orai mechanism, voltage-dependent calcium entry, inositol triphosphate receptor (IPR), endoplasmic reticulum (ER) flux, SERCA pump, and plasma membrane flux in our mathematical model. We use Green's function and Hankel and Laplace integral transforms to solve the membrane flux problem. Our simulations investigate the effects of various factors on the spatiotemporal behavior of calcium levels, with a simulation on the buffers in Alzheimer's disease-affected neurons. We also look at the effects of calcium-binding substances like the S100B protein and BAPTA and EGTA. Our results demonstrate how important the S100B protein Amyloid beta and the STIM-Orai mechanism are, and how important they are to consider when simulating the calcium signaling system. As such, our research indicates that a more realistic and complete model for modeling calcium dynamics may be obtained by using a generalized reaction-diffusion technique.

Keywords: Fractional-order derivative; calcium ions; neuron; Alzheimer's disease

AMS 2020 Classification: 35R11; 35A22; 35K57; 92C20

1 Introduction

Calcium ions Ca^{2+} serving as ubiquitous second messengers, play a crucial role in various cellular processes. These include cellular differentiation, excitability, apoptosis, gene transcription, and synaptic plasticity, all integral to maintaining cellular function and system regulation [1]. To regulate these diverse functions, cells employ multiple mechanisms to control intracellular

➤ **Received:** 14.07.2024 ➤ **Revised:** 28.10.2024 ➤ **Accepted:** 30.10.2024 ➤ **Published:** 31.10.2024

calcium levels. These mechanisms include the passive entry of calcium from the extracellular space through various voltage-gated and membrane ER pathways and diffusion within the cell, followed by sequestration by intracellular entities [2, 3]. Calcium enters the cell through voltage-operated calcium channels and certain exchangers. This diffusion triggers the immediate activation of physiological processes. A significant amount of calcium is buffered immediately, while the remainder undergoes further processing. The spatial and temporal dynamics of calcium inside neurons are essential for healthy cellular function, which can be analyzed by mathematical modeling.

The endoplasmic reticulum (ER) serves as a major internal calcium reservoir, playing a pivotal role in intracellular calcium signaling. The ER releases calcium, contributing to calcium waves that facilitate signaling cascades. Other factors, such as Plasma membrane calcium ATPase (PMCA), Orai channel, and mitochondria, are also actively involved in maintaining cytoplasmic calcium concentration.

Calcium diffuses within the cell through various pathways in cytosolic fluid and different organelles. This calcium homeostasis depending on various factors creates anomalous behavior of the previous concentration profile. To address this complexity, Caputo's differential framework is applied to the nonlocal nature of the reaction-diffusion model. Non-integer differential equation considered the previous memory to compute the current step, which gives a better realistic approach.

The calcium hypothesis has been studied and mathematically modeled over the past few decades. Smith et al. have analyzed the asymptotic behavior of calcium signaling using a steady-state analytical solution approach [4]. Dupont et al. have modeled calcium-induced calcium release of intracellular pools and verified their results with experimental data [5]. Dupont et al. developed a simplified model of the calcium kinase and its transductions [6]. Smith et al. examined several aspects of calcium kinetics, including oscillation patterns, buffer interactions, and receptor involvement [7]. Schmeitz et al. have investigated the time and space features of calcium signaling in T cells in a variety of experimental data systems [8]. The work of Friedhoff et al. was an analysis of the nature of calcium oscillations by means of stochastic methods [9]. The comprehensive study of bifurcation analysis of calcium oscillations was the focus of the work of Marko et al. [10]. In addition, Dave and Jha extended the studies by applying the models to Alzheimer's dementia and have shown aberrant calcium levels in nerve cells [11]. Manhas et al. have developed models for the evaluation of calcium bifurcation studies in acinar cells [12]. Naik and Pardasani worked out the finite element approach to calcium diffusion along with ER and the plasma membrane for the oocyte [13]. Jha et al. investigated the fractional calcium reaction-diffusion in nerve cells [14]. Joshi and Yavuz explored the bifurcation of calcium transients in hepatocyte cells [15]. Vora et al. developed one- and two-dimensional fractional calcium dynamics with Orai flow in neuronal cells [16, 17]. Joshi and Jha studied the mechanism of chaotic calcium behavior using the Hilfer operator on neuronal cells [18]. Vaishali and Adlakha studied the ATP-insulin-IP_3 regulating calcium homeostasis in pancreatic cells [19]. Luchko and Yamamoto developed the time-fractional diffusion wave model, which was solved using an analytical approach [20]. Pawar and Pardasani developed models to elucidate the dynamics of calcium, inositol triphosphate (IP_3), and amyloid-beta systems and shed light on cellular degeneration [21]. Lai et al. studied the regulation of calcium and buffer by calcium channels in cardiac myocytes [22]. Luchko et al. established the uniqueness and existence of the initial value and boundary fractional differential problem, which helps to derive the maximum principle [23]. Agarwal et al. studied the advection-diffusion process of calcium by using the Caputo-Fabrizio operator [24]. Tewari et al. have developed a computational model for the homeostasis of calcium and mitochondria [25]. Jagtap and Adlakha studied the dynamics of IP_3R and calcium in the hepatocyte [26]. Singh et al. studied the calcium signaling in the alpha

cells using a numerical approach [27]. Hardagna et al. studied the calcium diffusion in nerve cells in polar dimensions using fractional dynamics [28]. Jha et al. studied the fractional order investigation of the neuronal polar diffusion equation [29]. Joshi studied the COVID-19 dynamics with neuro-degeneration using memory impact [30]. Purohit et al. studied the fractional dynamics with the multi-order approach in physics [31]. Vaishali and Adlakha studied the system of calcium homeostasis in beta cells [32]. Naik et al. studied the flip bifurcation analysis of the chemical model in discrete time [33]. Manhas studied the IP_3 and calcium oscillations for mitochondria in non-excitable cells [34]. Kumar and Erturk studied the cholera disease by using the fractional differential numerical method [35]. Nakul et al. studied the calcium diffusion in cholangiocyte cells using the finite volume approach [36].

As of now, there is a dearth of comprehensive research exploring the collective impacts of the Membrane and the endoplasmic reticulum (ER) through mathematical modeling. This study seeks to bridge this gap by analyzing the combined effects of these parameters on calcium oscillations in neuronal cells.

2 Essential mathematical definitions

Definition 1 *Let a function $f \in C((0,T)\times(0,R))$ is continuous and differentiable in space and time where $(r,t) \in (0,R),(0,T)$ [37–40].*

Definition 2 *Let $n > 0, n \in \mathbb{R}_+$ and Riemann–Liouville fractional integration defined by [37]*

$$J^{\alpha} f(t) = \frac{1}{\Gamma(\alpha)} \int_0^t (t-\xi)^{(\alpha-1)} f(\xi)\, d\xi, \quad \alpha > 0,\ \alpha \in \mathbb{R}. \tag{1}$$

Definition 3 *Caputo fractional integration and differentiation is defined by [37],*

$$ {}_0^c D_t^{\alpha} f(t) = J^{m-\alpha} D^m f(t), \tag{2}$$

$$ {}_0^c D_t^{\alpha} f(t) = \frac{1}{\Gamma(m-\alpha)} \int_0^t (t-\xi)^{(m-\alpha-1)} f(\xi)^m\, d\xi, \quad \alpha > 0,\ \alpha \in \mathbb{R}+. \tag{3}$$

Definition 4 *The Mittag-Leffler function is defined by a non-negative variable parameter α, a real number parameter β, and a complex plane variable p [37, 41],*

$$E_{\alpha}(p) = \sum_{k=0}^{\infty} \frac{p^k}{\Gamma(\alpha k+1)}, \tag{4}$$

$$E_{\alpha,\beta}(p) = \sum_{k=0}^{\infty} \frac{p^k}{\Gamma(\alpha k+\beta)}, \tag{5}$$

and transforming by Laplace definition [41],

$$\mathcal{L}\{E_{\alpha,\beta}(zt^{\alpha})\} = \frac{s^{\alpha-1}}{s^{\alpha} \mp z}, \tag{6}$$

$$\mathcal{L}\{t^{\gamma-1}E_{\mu,\gamma}(\pm pt^{\mu})\} = \frac{s^{\mu-\gamma}}{s^{\mu} \mp p}, \quad Real(s) > \mid p \mid^{1/\mu},\ p \in \mathbb{C}, \tag{7}$$

$$\mathcal{L}\{{}_0^c D_t^{\alpha} f(t)\} = s^{\alpha} F(s) - \sum_{k=0}^{n-1} s^{\alpha-k-1} f^k(0), \quad n-1 < \alpha \le n. \tag{8}$$

Definition 5 *Wright's function, which is defined by [37],*

$$\phi(\alpha, \mu, p) = \sum_{k=0}^{\infty} \frac{p^k}{\Gamma(\alpha k + \mu) k!}, \quad \mu > -1, \ \mu \in \mathbb{C}, \tag{9}$$

and its Laplace transform is [41]

$$\mathcal{L}\{\phi(\alpha, \mu, -pt^{\mu})\} = s^{-1} e^{s^{\mu} p}. \tag{10}$$

Definition 6 *Mainardi's function [41] is given by,*

$$M_{\alpha}(p) = \sum_{k=0}^{\infty} \frac{-p^k}{\Gamma(-\alpha k + (1-\alpha)) k!}, \quad 0 < \alpha < 1. \tag{11}$$

Mainardi's function Laplace transform is

$$\mathcal{L}\left\{ t^{-\alpha} M_{\alpha}\left(\frac{p}{t^{\alpha}}\right)\right\} = s^{\alpha - 1} e^{-s^{\alpha} p}. \tag{12}$$

3 Modeling and biological background

A fractional model has been created to examine the influence of the Amyloid beta, STIM-Orai channel in conjunction with important factors such as buffer concentration, VGCC, IP_3 receptors, and ER fluxes. Subsequently, these components' responsibilities are examined to learn how they affect neuronal processes and diseases like Alzheimer's disease.

Impact of protein

Calcium ions interact and combine with protein resulting in calcium-bound buffers, which is a necessary step in modeling the spatiotemporal behavior of calcium ions. Entry of neurotransmitters between nerve cells depends on this calcium buffer reaction. Errors in this buffering mechanism have the potential to cause cell death and play a role in the emergence of neurodegenerative illnesses like Parkinson's and Alzheimer's disease.

The buffer complex is described using a chemical reaction equation. The mathematical equation for the buffer complex and cytosolic calcium ions is as follows [42],

$$[Ca^{2+}] + [P] \underset{k_-}{\overset{k_+}{\rightleftharpoons}} [CaP]. \tag{13}$$

$[Ca^{2+}]$ represents calcium-free ions, whereas $[P]$ is a protein that binds to calcium ions and creates a calcium-bound protein molecule bound via the k_+ rate. This both-way process dissociates the bound from calcium molecules and the protein at a disassociation rate of k_-.

Impact of amyloid beta

The distortion of amyloid precursor protein (APP) results in the production of amyloid beta 42 ($A\beta 42$), which perforates the plasma membrane. Amyloid beta plaques and tangles build up as a result, inhibiting surrounding plasma membrane processes. $A\beta 42$ opens up a new channel for calcium ions, causing the concentration of calcium to rise quickly to unmanageable levels without

a sustained influx. For weak neurons, the accumulating calcium is harmful [43]. Then we have

$$J_{Am} = V_{Am} \frac{1}{1 + e^{(V-q_1)/q_2}}, \tag{14}$$

where V_{Am} is the rate of calcium ions entering through this pathway. q_1 and q_2 are voltage dependence of calcium ions and values are -30,23 mV.

Impact of STIM-Orai

The development of memory carrier spines in neurons is mediated by the STIM-Orai pathway. The calcium ions that stream from the nanodomain of the Orai channel are made easier by STIM insights, which control calcium activity through ER calcium concentration. Calcium ions help mature mushroom spines maintain their steady shape. Any disruption of channel clusters or erratic flow might lead to cognitive impairments [44, 45],

$$J_{Orai} = \phi \frac{I_{Orai}}{A_O z F}. \tag{15}$$

In this context, ϕ represents the probability of channel opening, I_{Orai} denotes the current flowing through the Orai channel.

Impact of IP_3R

The main intracellular calcium storage is located in the ER. IP_3 receptors (IP_3R) have the ability to release calcium, which is controlled by the biphasic connection between calcium and inositol 1,4,5-trisphosphate (IP_3). Intracellular calcium oscillations are induced by IP_3R flow and are necessary for processes such as synaptic modulation, learning, and neurite development. The intraorganellar network's calcium homeostasis can be both elevated and disrupted by mutations [11],

$$J_{IP_3R} = (C_{ER} - C) K_{IP_3R} O_{IP_3R}. \tag{16}$$

C_{ER} is the calcium level in ER, C is cytosolic calcium, and O_{IP_3R} is the opening rate of the IPR, which varies from zero to one.

Impact of SERCA

The Sarcoendoplasmic Reticulum Calcium ATPase (SERCA) pump is a component of the ER calcium store replenishment system that attenuates cytoplasmic calcium signal hyperactivity. Calcium sequestration systems may be severely overloaded by a modified SERCA pump [46],

$$J_{SERCA} = V_{SERCA} \frac{C^2}{C^2 + K_{SERCA}^2} \frac{1}{C_{ER}}. \tag{17}$$

V_{SERCA} is pump value, K_{SERCA} is the dissociation factor of pump.

Impact of channel and leak flux

Calcium moves passively from the endoplasm into the cytoplasm via channels and leaks made of different kinds of pores and proteins. Calcium homeostasis can be upset and the ER overloaded

by poor calcium control. The mathematical formulation of leak and channel flow is as follows [46],

$$J_{leak} = \frac{D_{leak}}{C_1}(1+C_1)\left(\frac{C_0}{1+C_1} - C\right), \tag{18}$$

$$J_{Ch} = \frac{D_{Chan}}{C_1}(1+C_1)\left(\frac{C_0}{1+C_1} - C\right), \tag{19}$$

where D_{leak} is leak constant, D_{Chan} is channel conductance.

Impact of PMCA flux

Via the high-energy, high-affinity PMCA pump, which the tau protein may block, the plasma membrane actively mediates calcium and dysregulates cytoplasmic calcium. This disturbance is quantitatively represented by the mathematical expression of PMCA flux [46],

$$J_{PMCA} = V_{PMCA}\frac{C^2}{C^2 + K_{PMCA}^2}. \tag{20}$$

Impact of voltage-dependent calcium channel

Calcium ion channels that are gated by voltage are present in neurons and other excitable cells. These ion channels allow the movement of ions, such as sodium, chloride, and calcium, into and out of the cells. VDCC plays a crucial role in the influx of calcium into cells, which then triggers various intracellular physiological processes [47, 48]. VDCCs are categorized into these subtypes $L, P/Q, N$, and T subtypes. L-type calcium channels are of particular importance in brain cells, initiating calcium-based activities and subsequent intracellular processes. This equation is expressed as follows [46, 49],

$$I_{VDCC} = P_V z^2 \frac{F^2 V_m}{RT}\frac{C - Ca_o exp(-z\frac{FV_m}{RT})}{1 - exp(-z\frac{FV_m}{RT})}, \tag{21}$$

calcium flux is given by,

$$\sigma_{Ca} = \frac{-I_{Ca}}{V_{neurons} z F}. \tag{22}$$

Table 1 shows all of the values for these parameters.

Modified model in Caputo sense

By combining channels, leaks, pumps, and buffer reactions, one may represent simplified neuronal calcium homeostasis by converting the time derivative into a Caputo fractional derivative. The following is how the suggested model is put forth:

$$\frac{\partial^u C}{\partial t^u} = D\left(\frac{\partial^2 C}{\partial r^2} + \frac{1}{r}\frac{\partial C}{\partial r}\right) - k_+[P][Ca^{2+}] + k_-[CaP] + J_{IPR} - J_{SERCA} + J_{leak} + J_{Ch}. \tag{23}$$

The other formulations, as is customary, represent the order of the Caputo derivative, u, which has a lower limit equal to zero and an upper limit equal to t.

The initial condition and boundary condition for the derivation of the above formula are as follows

$$C(r,0) = g(r), \quad C(\infty,t) = 0. \tag{24}$$

As follows, the Neumann condition refers to the natural state of calcium diffusion in nerve cells

$$\frac{\partial[C]}{\partial n} = J_{Am} + J_{Orai} - J_{PMCA} + J_{VDCC}. \tag{25}$$

To handle simple multiplication of the nonlinearity in J_{SERCA}. Linearizing the equation by taking two different possible aspects [50]:
Case 1: For $C \ll K_{SERCA}$. Then

$$\frac{C^2}{C^2 + K_{SERCA}^2} \ll \frac{C^2}{K_{SERCA}^2} \ll \frac{C}{K_{SERCA}}. \tag{26}$$

Case 2: For $K_{SERCA} \ll C$. Let $K = \beta c$, for $0 < \beta < 1$,

$$\frac{C^2}{C^2 + K_{SERCA}^2} = \frac{1}{1+\beta^2}. \tag{27}$$

Nondimensionalization for the term of the proposed model is as follows:

$$r^* = r/l, \quad t^* = t/T, \quad C^* = C/K, \quad C_\infty^* = C_\infty/K, \quad P_\infty^* = P_\infty/[P]_T.$$

To decrease the complexities of the following model, which is the proposed mathematical form, and let

$$a = k_+[P] - K_{IPR}O_{IPR} + \frac{K_{SERCA}}{V_{SERCA}} - \frac{1+C_1}{C_1}(D_{leak} + D_{Chan}),$$

$$b = k_+[P]C_\infty + C_{ER}(K_{IPR}O_{IPR}) + k_+[P]C_\infty + (D_{leak} + D_{Chan})[C_0/C_1],$$

$$\overset{C}{_0}D_t^u C = D_{Ca}\nabla^2 C - a_i C + b_i, \tag{28}$$

where i = 1, 2 for Case 1 and Case 2, respectively.

4 Main results

In this section, the solution of the calcium diffusion fractional dynamics is solved by using the hybrid transform method.

Theorem 1 *For variables of the range, $0 \le t < \infty$, $0 \le r < \infty$, $u = (0,1]$, have the form as Eq. (28) and basic condition as Eq. (24), Neuronal calcium flow comes from various channels and receptors which are considered a non-homogeneous condition, (25), can be derived as the form,*

$$G(r,t) = \frac{\sqrt{2}}{\sqrt{\pi}}\int_0^\infty E_u[(Dk^2 - a_i)t^u]J_0(kr)kdk + \frac{\sqrt{2}}{\sqrt{\pi}}(b_i + j_o)t^u\int_0^\infty E_{u,u+1}[(Dk^2 - a_i)t^u]J_0(kr)kdk. \tag{29}$$

Proof Using Eq. (28) as our foundational model.
Taking two cases for the SERCA pump, v. The Hankel transform is applied over the radius.

$$ {}_0^C D_t^u \dot{C} = Dk^2 \dot{C} - a_i \dot{C} + (b_i + j_0)\delta(k), \tag{30} $$

using the Laplace transform to apply temporal transformation

$$ \ddot{C}(k,s) = \frac{s^{u-1} g(\dot{k})}{(s^u - Dk^2 + a_i)} + \frac{b_i + j_o \delta(k)}{s(s^u - Dk^2 + a_i)} \delta(k), \tag{31} $$

where k is the Hankel transform variable.
The Laplace transform is now used by the formulas below in the solution

$$ \begin{aligned} E_u(pt^u) &\leftarrow L \rightarrow \frac{s^{u-1}}{s^u - p}, \\ t^{\gamma-1} E_{u,\gamma}(pt^u) &\leftarrow L \rightarrow \frac{s^{\mu-1}}{s^\mu \mp p}, \end{aligned} \tag{32} $$

$$ C(\dot{k},t) = E_u[(Dk^2 - a_i)t^u] g(\dot{k}) + (b_i + j_o) t^u E_{u,u+1}[(Dk^2 - a_i)t^u]\delta(k). \tag{33} $$

With the inverting transform, we obtain:

$$ \begin{aligned} C(r,t) &= \frac{\sqrt{2}}{\sqrt{\pi}} \int_0^\infty E_u[(Dk^2 - a_i)t^u] g(\dot{k}) J_0(kr) k dk \\ &\quad + \frac{(b_i + j_o)t^u \sqrt{2}}{\sqrt{\pi}} \int_0^\infty E_{u,u+1}[(Dk^2 - a_i)t^u]\delta(k) J_0(kr) k dk, \end{aligned} \tag{34} $$

$$ \begin{aligned} C(r,t) &= \frac{\sqrt{2}}{\sqrt{\pi}} \int_0^\infty E_u[(Dk^2 - a_i)t^u] J_0(kr) k \int_0^\infty g(y) J_0(kr) k dy * dk \\ &\quad + \frac{(b_i + j_o)t^u \sqrt{2}}{\sqrt{\pi}} \int_0^\infty E_{u,u+1}[(Dk^2 - a_i)t^u] \int_0^\infty \delta(y) J_0(kr) k dy * dk, \end{aligned} \tag{35} $$

$$ C(r,t) = \int_0^\infty G^1(r-y,t) g(y) dy + \int_0^\infty G^2(r-y,t)\delta(y) dy. \tag{36} $$

$$ G_u^1(r,t) = \frac{\sqrt{2}}{\sqrt{\pi}} \int_0^\infty E_u[(Dk^2 - a_i)t^u] J_0(kr) k dk, \tag{37} $$

$$ G_u^2(r,t) = (b_i + j_o)t^u \int_0^\infty E_{u,u+1}[(Dk^2 - a_i)t^u] J_0(kr) k dk, \tag{38} $$

$$ \begin{aligned} G_u(r,t) &= \frac{\sqrt{2}}{\sqrt{\pi}} \int_0^\infty E_u[(Dk^2 - a_i)t^u] J_0(kr) k dk \\ &\quad + \frac{\sqrt{2}}{\sqrt{\pi}} (b_i + j_o)t^u \int_0^\infty E_{u,u+1}[(Dk^2 - a_i)t^u] J_0(kr) k dk. \end{aligned} \tag{39} $$

Hence proved.

Lemma 1 *[38–40] An example of a function with an exponential combination is the Mittag-Leffler function family. When $Z \in C$, a complex field, has any value, $E_{(\mu,\gamma)}(x)$ converges. Eq. (40) is a Green's function*

solution derived by a semi-analytical method for calcium diffusion in neuron cells. This analytical method, however, needs to be revised to provide closed-form answers.

5 Analysis

The essential solution was obtained by using Green's function to describe the outcome of the integral transform. Below is the further analysis that was performed to get a closed-form answer.

Theorem 2 *Taking* $0 < u \leq 1$, $0 < r < \infty$, $0 \leq t < \infty$, *the mathematical form is* (40) *from this closed-form solution obtained as,*

$$G(r,t) = \frac{1}{2D\sqrt{t^u}} \int_0^\infty e^{\frac{-r^2}{4t^u k} - a_i k t^u} k^{-\frac{1}{2}} M_u(k) dk + \frac{(b_i + j_o)t^{u/2}}{2D} \int_0^\infty e^{\frac{-r^2}{4t^u k} - a_i k t^u} k^{-\frac{1}{2}} \phi(-u, 1; k) dk. \quad (40)$$

Proof Implementing the Hankel transform to a radial variable and using Eq. (40), we obtain,

$$G_u(r,t) = E_u[(Dk^2 - a_i)t^u] + (b_i + j_o)t^u E_{u,u+1}[(Dk^2 - a_i)t^u]. \quad (41)$$

Now using the Laplace to transform the temporal domain, we obtain,

$$\ddot{G_{u,2}}(k,s) = \frac{s^{u-1}}{(s^u + Dk^2 + a_i)} + \frac{s^{-1}(b_i + j_o)}{(s^u + Dk^2 + a_i)}, \quad (42)$$

$$\ddot{G_{u,2}}(k,s) = s^{u-1} \int_0^\infty e^{-p(s^u + Dk^2 + a_i)} dp + (b_i + j_o)s^{-1} \int_0^\infty e^{-p(s^u + Dk^2 + a_i)} dp. \quad (43)$$

Applying the inverse Laplace now, and utilizing the definitions,

$$\ddot{G_{u,2}}(k,s) = \int_0^\infty e^{-p(Dk^2 + a_i)} t^{-u} M_u\left(\frac{p}{t^u}\right) dp + (b_i + j_o) \int_0^\infty e^{-p(Dk^2 + a_i)} \phi(-u, 1; -pt^u) dp. \quad (44)$$

Using the inverse Hankel transform, we get

$$G(r,t) = \frac{1}{2D\sqrt{t^u}} \int_0^\infty e^{\frac{-r^2}{4t^u k} - a_i k t^u} k^{-\frac{1}{2}} M_u(k) dk + \frac{(b_i + j_o)t^{u/2}}{2D} \int_0^\infty e^{\frac{-r^2}{4t^u k} - a_i k t^u} k^{-\frac{1}{2}} \phi(-u, 1; k) dk. \quad (45)$$

Hence the result.

Existence and uniqueness

Remark 1 *[38, 39] The closed-form solution is gained by using Green's function.*
Let $\alpha, m > 0$, *then for* p, *continuous function defined below*

$$E_{(m,\alpha)}(p) = \sum_{k=0}^{\infty} p^k / (m(\mu k + \mu)), \quad (46)$$

is the convergent and let constant $M_i > 0$ *as,*

$$| E_{(m,\mu)}(z) | \leq M_i. \quad (47)$$

If $\alpha \geq 0$ *and* $\xi \in C$, *thus additions of the above series uniformly converge throughout an entire complex plane [39, 40].*

For the uniqueness of the solution, let us take $c(r,t) = h(r,t) - \dot{h}(r,t)$. *If a distinguished result exists of this nature with this physiological constraint then* $c(r,t) \equiv 0 \rightarrow h(r_i,t_i) \equiv \dot{h}(r_i,t_i)$ *which shows the uniqueness of the solution.*

Theorem 3 $c \in C[[0,T] \times [0,R]]$ *and states the Eq. (28), equality can be given as below,*

$$max_{\Omega} c = max_{\Gamma} c, \tag{48}$$

where Γ *is the boundary and* Ω *is the domain.*

Proof This statement will be proven by contradiction.
Let us take into consideration

$$M = max_{\Omega} c, \tag{49}$$
$$\ddot{M} = max_{\Gamma} c, \tag{50}$$

concerning this $\ddot{M} \leq M$. Then M carries any arbitrary point (r_M, t_M).
Using a function that can be expressed as $w : \Omega \rightarrow \mathbb{R}$ fulfills our assumption as well, having equivalent physiological values.
Now, we may proceed as follows

$${}_0^C D_t^u w - D\nabla^2 w + a_i w - b_i = 0, \tag{51}$$

considering the function as it is described here

$$w = c + (M - \ddot{M}) t^{(-m)}. \tag{52}$$

In maximal attainment at a level of c. (r_M, t_M) above equation implies

$$w = \ddot{M} + (M - \ddot{M})\epsilon, w < M. \tag{53}$$

Also, $w \geq c$ in Ω and at maximum point

$$w = c(r_M, t_M) + M - \ddot{M}. \tag{54}$$

For the left-side equation

$${}_0^C D_t^u w - D\frac{\partial^2 w}{\partial r^2} + \frac{1}{r}\frac{\partial w}{\partial r} + a_i w - b_i + \frac{M - \ddot{M}\Gamma(1-m)}{\Gamma(1-m-u)} t^{-m-u} \leq \frac{M - \ddot{M}\Gamma(1-n)}{\Gamma(1-m-u)} t^{-m-u} > 0. \tag{55}$$

From above equation

$${}_0^C D_t^u c - D\nabla^2 c + a_i c - b_i > 0. \tag{56}$$

The positive output contradicts this

$$max_{\Omega} c = max_{\Gamma} c. \tag{57}$$

Hence proved.

Applicability of the model

A multitude of cerebral processes, including neurotransmitter release, synaptic plasticity, and gene transcription, are contingent upon calcium ions. To achieve physiological equivalence with in vivo neuronal calcium dynamics, the calcium amounts in our model were adjusted. This method ensures that the model accurately mimics the behavior of neuronal calcium.

A variety of brain processes, including neurotransmitter release, synaptic plasticity, and gene transcription, are critically dependent upon calcium ions. In order to achieve physiological equivalence with in vivo neuronal calcium dynamics, the calcium amounts in the model were adjusted. This ensures that the model accurately mimics the behavior of neuronal calcium [14, 18].

6 Results and interpretation

The results demonstrate the distribution of calcium within a neuron in terms of spatial and temporal dimensions. Table 1 provides the numerical values and accompanying descriptions of the input parameters utilized in the generation of these results.

In Figure 1, shows the calcium pattern for a $100\mu M$ buffer. This graphic depicts the creation of a calcium spike that is uniformly distributed in terms of temporal order transition for the cytosol. This hysteresis memory emphasizes the nonlocal character of neuronal calcium transport at a scale of $0.7\mu M$. Calcium ions diffuse across the cytosolic buffer, binding to the ER storage receptors and profoundly altering protein activity. Calcium ion concentration falls linearly as the radial distance from the plasma membrane increases. Buffer is very important in calcium homeostasis. We can observe the temporal impact on the calcium ions with differential order. Here EGTA buffer is taken for normal neuronal cells which are bound with the calcium ions.

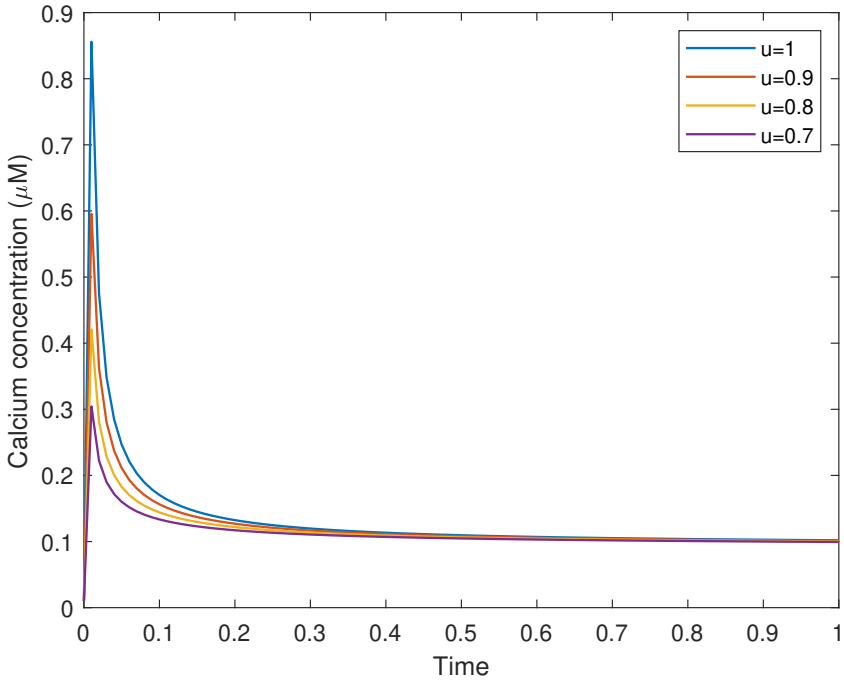

Figure 1. The time diffusion of calcium ions, as simulated by successive orders of the time derivative, when the buffer is 100 μM

In Figure 2, shows the radial distribution of calcium concentration at a buffer value of 100 μM with a fractional order $u = 1, 0.9, 0.8, 0.7$. This illustration depicts the creation of a calcium spike

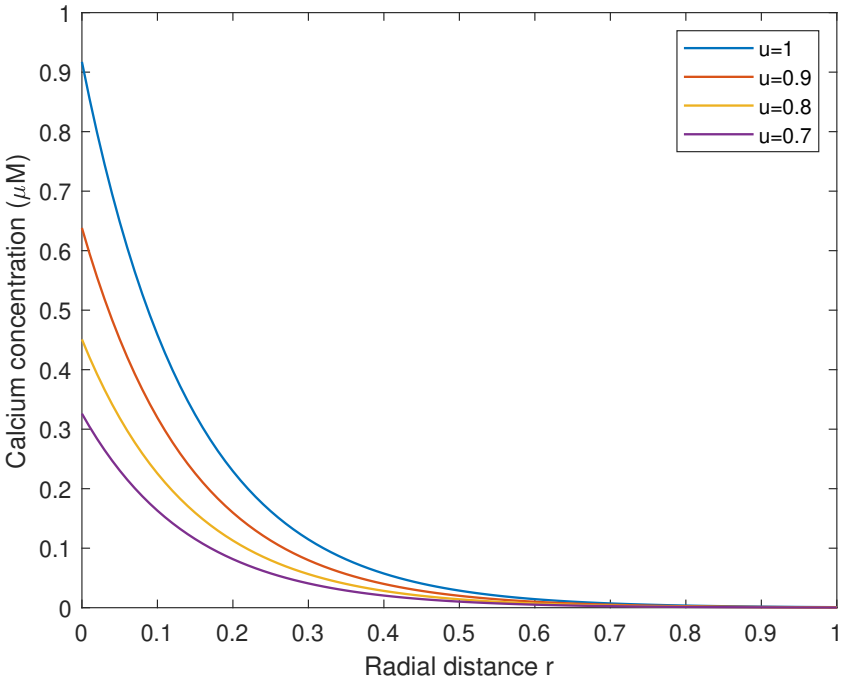

Figure 2. The radial distribution of calcium ions, as simulated by successive orders of the time derivative, when the buffer is 100 μM

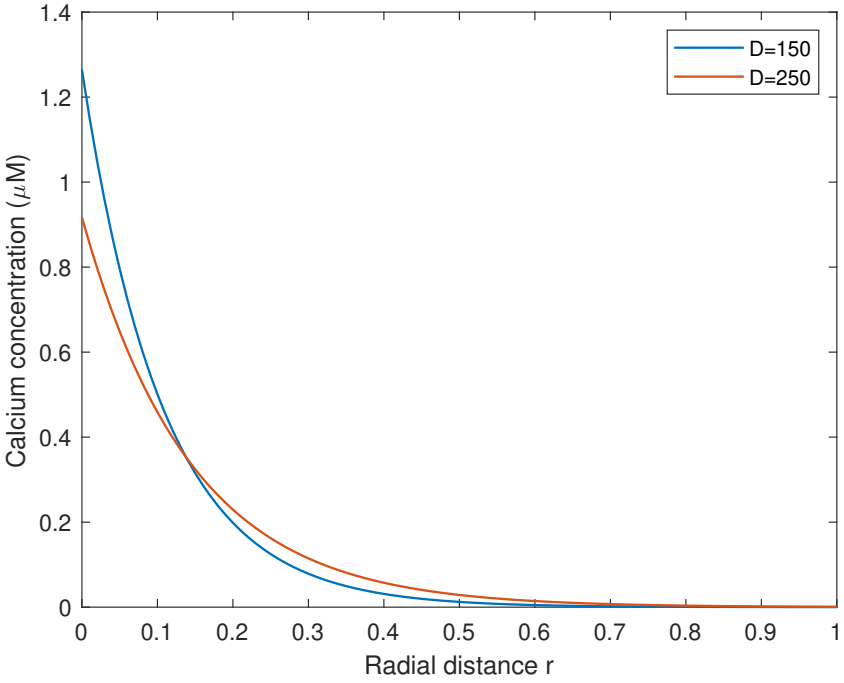

Figure 3. Radial distribution of free calcium ions for a diffusion coefficient 150 and 250 with temporal order $u = 1$

dispersed radially in the cytosolic free calcium concentration. At $u = 0.9$, the hysteresis memory has a lower nonlocal character than $u = 1.0$. The lower fractional order $u = 0.9$ results in a reduction in cytosolic free calcium ions, creating a subdiffusion impact on the spatial pattern. This order includes all prior states up to 0.9 of the reaction-diffusion process, recording the transition

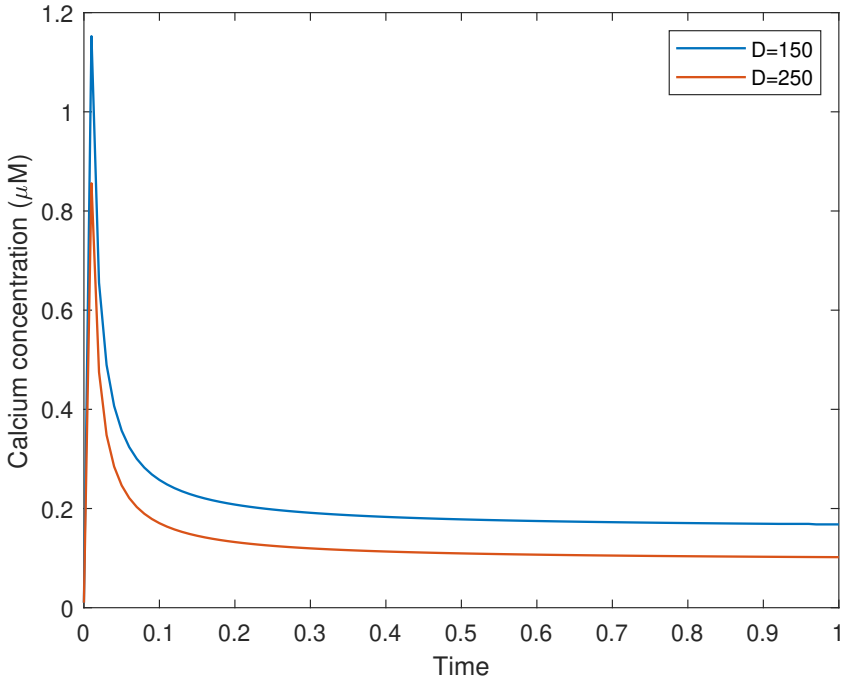

Figure 4. Temporal pattern of free calcium ions for a diffusion coefficient 150 and 250 with temporal order $u = 1$

of the differential order of calcium ions.

In Figure 3, displays calcium concentration variations with a diffusion coefficient of $D = 150$ for this reaction-diffusion process with radial distance. $D = 250$ shows that calcium concentration increases with a reduced diffusion coefficient, signifying localized calcium signaling locations and probable calcium overload.

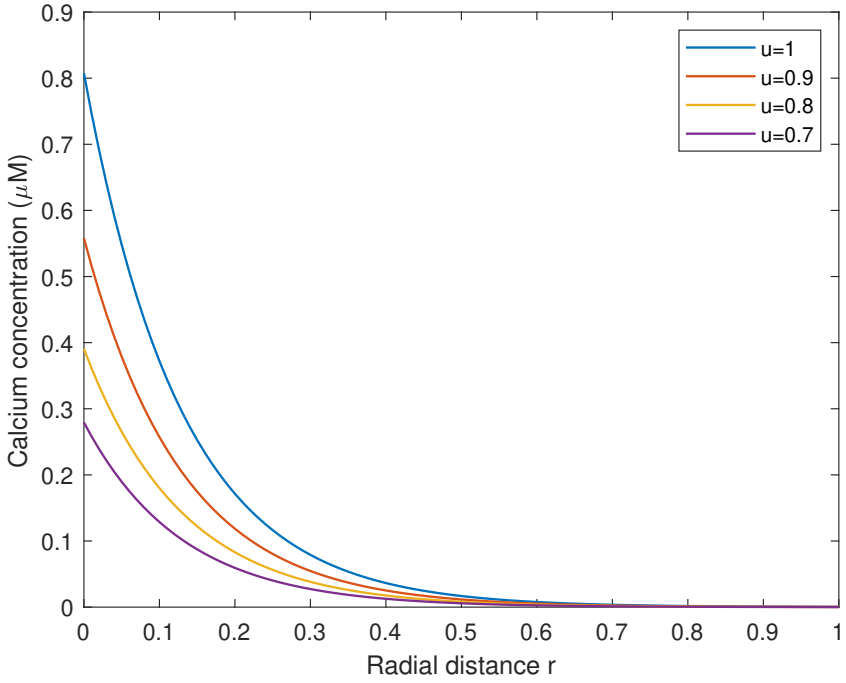

Figure 5. Radial diffusion of calcium ions with $[B] = 200\mu M$ for a different order of time derivative

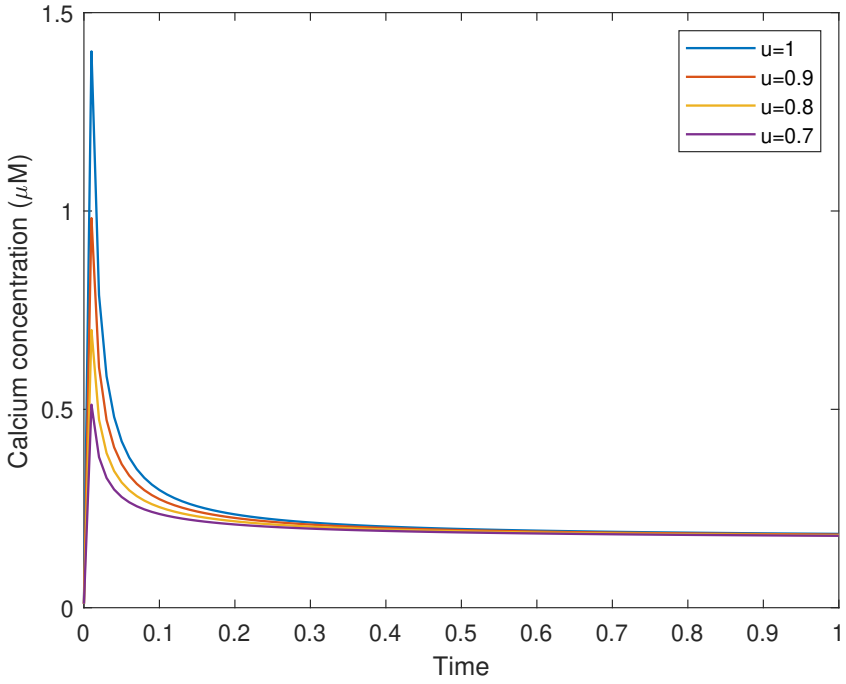

Figure 6. Temporal pattern in Alzheimer's impact of reduced protein $[B] = 50\mu M$ on calcium ions for a different order

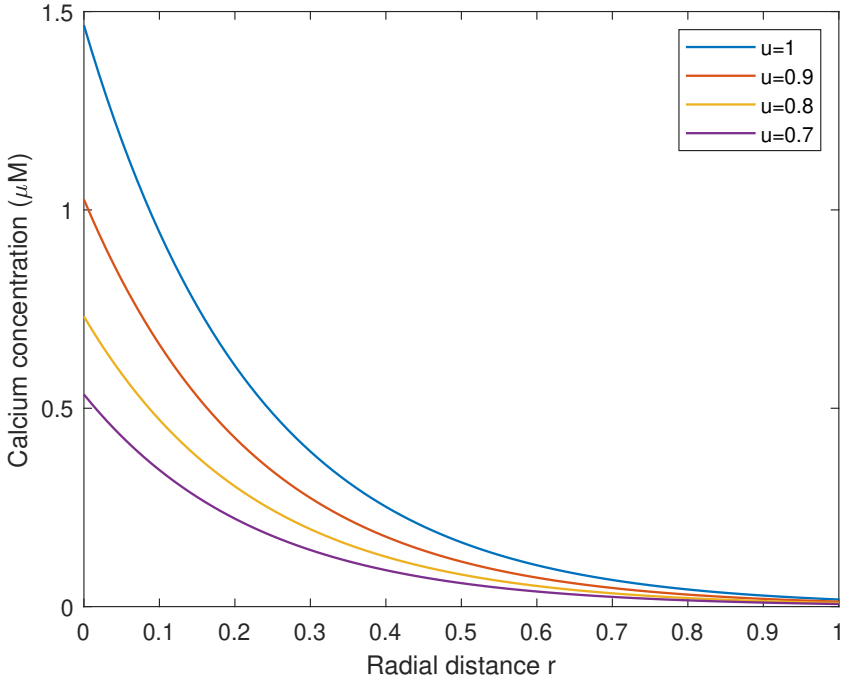

Figure 7. Radial distribution in Alzheimer's impact of reduced protein $[B] = 50\mu M$ on calcium ions for a different order

Figure 4 displays calcium concentration variations with a diffusion coefficient of $D = 150$ for this fractional temporal reaction-diffusion process. $D = 250$ shows that calcium concentration

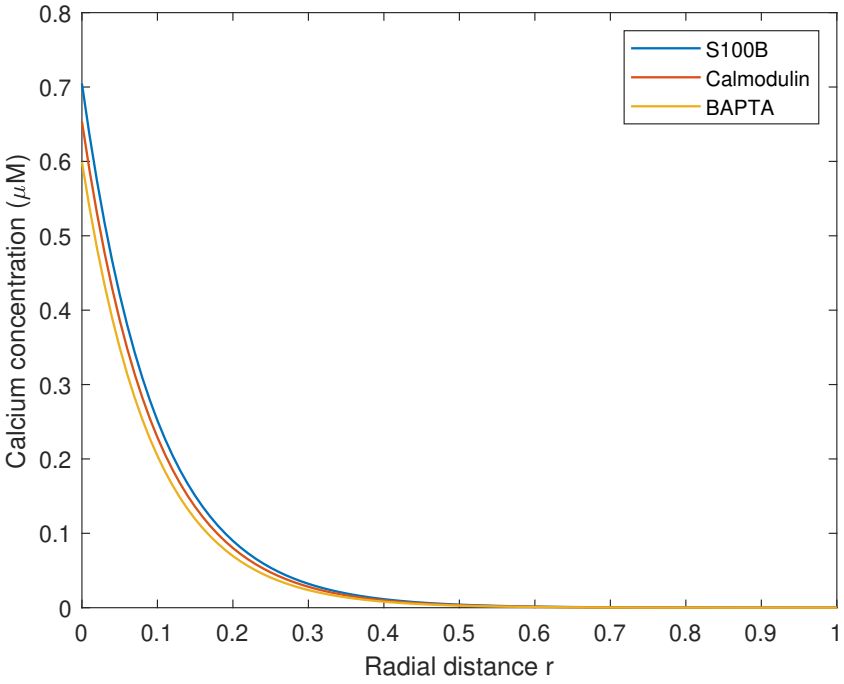

Figure 8. Radial distribution of free calcium ions for various protein impact

increases with a reduced diffusion coefficient, signifying intersection indicates the background calcium level decreased.

In Figure 5, we show calcium concentration with increasing buffer concentration $[B] = 200\mu M$ along the radius. The figure shows that the calcium spectrum is controlled, with enhanced calcium binding activity, showing that increasing buffer concentrations effectively regulate calcium levels.

In Figure 6, we illustrate the effect of the reduced buffer presence observed in Alzheimer's impacted neurons. This can increase the amount of calcium ions, degenerating neuronal homeostasis and leading to neuronal death. The temporal pattern is higher than the normal neuronal cell.

In Figure 7, it illustrates the effect of the reduced buffer presence observed in the radial distance with different temporal order. It can be observed that calcium spread and peak levels are higher and prolonged than normal neuronal conditions. Long-term calcium behavior is harmful to neurons, which leads to cell death.

In Figure 8, it illustrates the nature of the endogenous buffer calmodulin, S100B can control the calcium spectrum in a well-controlled manner. The presence of the BAPTA buffer in the cytosol could disperse calcium in a narrow spectrum. This effect can be useful for well-controlled calcium dispersion in the Alzheimer's impacted neuron.

Table 1. Values of physiological constants [4, 9, 43]

Symbols	Description	Value	Unit
D_{Ca}	Diffusion constant value	150-250	$\mu M^2/s$
C_1	Cell ratio	0.185	-
k_+	Association constant rate (EGTA, S100B, BAPTA)	1.5,1.1,600	$\mu M^{-1}s^{-1}$
$[Ca^{2+}]_\infty$	Background concentration level	0.1	μM
V_{SERCA}	Pump conductance	120	$s^{-1}(\mu M)^{-2}$
D_{leak}	Leak flux constant	0.11	s^{-1}
D_{Chan}	Channel flux constant	6	s^{-1}

[P]	Protein level	50-100	μM
ϕ	Opening rate	0.9	-
I_O	Current of Orai	2.1	fA
A_O	Area of Orai	0.25	nm^2
z	Valency of calcium ions	2	-
C_0	extracellular calcium concentration	2	μM
V_{neuron}	Volume of cellular cytosol	523.6	μm^3
V_m	membrane potential	-0.07	V
R	Ideal gas constant	8.31	J/(mol.K)
T	Absolute temperature	300	K
P_V	Permeability of ion	0.5	s^{-1}
K_{SERCA}	Dissociation SERCA rate	0.18	μM
K_{PMCA}	PMCA pump rate	0.425	μM
C_{ER}	ER calcium level	500	μM
V_{PMCA}	PMCA conductance	28	$s^{-1}(\mu M)^{-2}$
K_{IP_3R}	IPR rate	0.52	s^{-1}

7 Conclusion

In this work, we have simulated the interaction of calcium ions and buffers with temporal fractional order, taking into account a variety of characteristics including neuronal membrane flux and ER flux. Different endogenous and exogenous proteins have been investigated in the context of Alzheimer's disease. The Hankel transform has been used for the polar derivative and the Laplace transform for initial conditions, resulting in Mittag-Leffler functions. Green's functions have been used to obtain closed-form solutions, which have also included Mainardi's and Wright's functions. A modified calcium diffusion model, formulated within the Caputo framework, has been successfully solved through a hybrid transform method. The existence and uniqueness of the solution have been demonstrated for fundamental model analysis.

- We have obtained graphical results of the interaction of calcium and other factors with different temporal order, reduced temporal memory reduced the calcium level in neurons.
- The study shows that the time fractional order has a converging effect on calcium levels for radial distance, driven by many characteristics.
- The diffusion coefficient parameter has an inverse influence on calcium distribution, causing calcium concentrations to accumulate near the membrane.
- The impact of Alzheimer's disease is demonstrated by a reduced buffer quantity, resulting in prolonged elevated calcium levels in neurons, which are hazardous. Prolonged conditions could lead to cell death with lower buffer impact.
- Neuroprotection relies heavily on BAPTA binding concentration. Mobile and immobile buffers have distinct effects on calcium levels, with EGTA, Calmodulin, and S100B considerably lowering calcium concentrations.

Thus, our findings provide light on the fractional dynamics of calcium signaling and buffering in neurons, offering insights into protein simulation possibilities for neurodegenerative illnesses such as Alzheimer's. The dual transform approach and fractional-order modeling provide a solid foundation for comprehending the intricate interconnections seen in the neural calcium reaction-diffusion process.

Limitation and future scope

In this work, the experimental setup could play a pivotal role in the understanding of neuronal degenerative diseases.

Declarations

Use of AI tools

The authors declare that they have not used Artificial Intelligence (AI) tools in the creation of this article.

Data availability statement

All data generated or analyzed during this study are included in this article.

Ethical approval

The authors state that this research complies with ethical standards. This research does not involve either human participants or animals.

Consent for publication

Not applicable

Conflicts of interest

The authors declare that they have no conflict of interest.

Funding

There is no funding for this article.

Author's contributions

B.K.J.: Conceptualization, Formal Analysis, Writing-Original Draft. V.H.V.: Methodology, Visualization, Validation, Writing - Review & Editing. T.P.S.: Validation, Writing-Original Draft. The authors have read and agreed to the published version of the manuscript.

Acknowledgements

Not applicable

References

[1] Workgroup, A.A.C.H and Khachaturian, Z.S. Calcium hypothesis of Alzheimer's disease and brain aging: a framework for integrating new evidence into a comprehensive theory of pathogenesis. *Alzheimer's & Dementia,* 13(2), 178-182, (2017). [CrossRef]

[2] Ribe, E.M., Serrano-Saiz, E., Akpan, N. and Troy, C.M. Mechanisms of neuronal death in disease: defining the models and the players. *Biochemical Journal,* 415(2), 165-182, (2008). [CrossRef]

[3] Bezprozvanny, I. Calcium signaling and neurodegenerative diseases. *Trends in Molecular Medicine,* 15(3), 89-100, (2009). [CrossRef]

[4] Smith, G.D. Analytical steady-state solution to the rapid buffering approximation near an open Ca^{2+} channel. *Biophysical Journal,* 71(6), 3064-3072, (1996). [CrossRef]

[5] Dupont, G., Berridge, M.J. and Goldbeter, A. Signal-induced Ca^{2+} oscillations: properties of a model based on Ca^{2+}-induced Ca^{2+} release. *Cell Calcium,* 12(2-3), 73-85, (1991). [CrossRef]

[6] Dupont, G., Houart, G. and De Koninck, P. Sensitivity of CaM kinase II to the frequency of Ca^{2+} oscillations: a simple model. *Cell Calcium,* 34(6), 485-497, (2003). [CrossRef]

[7] Sherman, A., Smith, G.D., Dai, L. and Miura, R.M. Asymptotic analysis of buffered calcium diffusion near a point source. *SIAM Journal on Applied Mathematics,* 61(5), 1816-1838, (2001). [CrossRef]

[8] Schmeitz, C., Hernandez-Vargas, E.A., Fliegert, R., Guse, A.H. and Meyer-Hermann, M. A mathematical model of T lymphocyte calcium dynamics derived from single transmembrane protein properties. *Frontiers in Immunology,* 4, 277, (2013). [CrossRef]

[9] Friedhoff, V.N., Ramlow, L., Lindner, B. and Falcke, M. Models of stochastic Ca^{2+} spiking. *The European Physical Journal Special Topics,* 230, 2911-2928, (2021). [CrossRef]

[10] Marhl, M., Haberichter, T., Brumen, M. and Heinrich, R. Complex calcium oscillations and the role of mitochondria and cytosolic proteins. *BioSystems,* 57(2), 75-86, (2000). [CrossRef]

[11] Dave, D.D. and Jha, B.K. Analytically depicting the calcium diffusion for Alzheimer's affected cell. *International Journal of Biomathematics,* 11(7), 1850088, (2018). [CrossRef]

[12] Manhas, N., Sneyd, J. and Pardasani, K.R. Modelling the transition from simple to complex Ca^{2+} oscillations in pancreatic acinar cells. *Journal of Biosciences,* 39(3), 463-484, (2014). [CrossRef]

[13] Naik, P.A. and Pardasani, K.R. Finite element model to study calcium distribution in oocytes involving voltage gated Ca^{2+} channel, ryanodine receptor and buffers. *Alexandria Journal of Medicine,* 52(1), 43–49, (2016). [CrossRef]

[14] Jha, B.K., Joshi, H. and Dave, D.D. Portraying the effect of calcium-binding proteins on cytosolic calcium concentration distribution fractionally in nerve cells. *Interdisciplinary Sciences: Computational Life Sciences,* 10, 674-685, (2018). [CrossRef]

[15] Joshi, H. and Yavuz, M. Numerical analysis of compound biochemical calcium oscillations process in hepatocyte cells. *Advanced Biology,* 8(4), 2300647, (2024). [CrossRef]

[16] Vatsal, V.H., Jha, B.K. and Singh, T.P. To study the effect of ER flux with buffer on the neuronal calcium. *The European Physical Journal Plus,* 138, 494, (2023). [CrossRef]

[17] Vatsal, V.H., Jha, B.K. and Singh, T.P. Deciphering two-dimensional calcium fractional diffusion of membrane flux in neuron. *Journal of Applied Mathematics and Computing,* 70, 4133–4156, (2024). [CrossRef]

[18] Joshi, H. and Jha, B.K. Chaos of calcium diffusion in Parkinson's infectious disease model and treatment mechanism via Hilfer fractional derivative. *Mathematical Modelling and Numerical Simulation with Applications,* 1(2), 84-94, (2021). [CrossRef]

[19] Vaishali and Adlakha, N. Model of calcium dynamics regulating IP_3, ATP and insulin production in a pancreatic β-cell. *Acta Biotheoretica,* 72, 2, (2024). [CrossRef]

[20] Luchko, Y., Mainardi, F. and Povstenko, Y. Propagation speed of the maximum of the fundamental solution to the fractional diffusion–wave equation. *Computers & Mathematics with Applications,* 66(5), 774-784, (2013). [CrossRef]

[21] Pawar, A. and Pardasani, K.R. Computational model of interacting system dynamics of calcium, IP_3 and β-amyloid in ischemic neuron cells. *Physica Scripta,* 99(1), 015025, (2024). [CrossRef]

[22] Lai, Y.M., Coombes, S. and Thul, R. Calcium buffers and L-type calcium channels as modulators of cardiac subcellular alternans. *Communications in Nonlinear Science and Numerical Simulation*, 85, 105181, (2020). [CrossRef]

[23] Luchko, Y. and Yamamoto, M. General time-fractional diffusion equation: some uniqueness and existence results for the initial-boundary-value problems. *Fractional Calculus and Applied Analysis*, 19(3), 676-695, (2016). [CrossRef]

[24] Agarwal, R., Kritika and Purohit, S.D. Mathematical model pertaining to the effect of buffer over cytosolic calcium concentration distribution. *Chaos, Solitons & Fractals*, 143, 110610, (2021). [CrossRef]

[25] Tewari, S.G., Camara, A.K.S., Stowe, D.F. and Dash, R.K. Computational analysis of Ca^{2+} dynamics in isolated cardiac mitochondria predicts two distinct modes of Ca^{2+} uptake. *The Journal of Physiology*, 592(9), 1917-1930, (2014). [CrossRef]

[26] Jagtap, Y. and Adlakha, N. Numerical model of hepatic glycogen phosphorylase regulation by nonlinear interdependent dynamics of calcium and IP_3. *The European Physical Journal Plus*, 138, 399, (2023). [CrossRef]

[27] Singh, T. and Adlakha, N. Numerical investigations and simulation of calcium distribution in the alpha-cell. *Bulletin of Biomathematics*, 1(1), 40-57, (2023). [CrossRef]

[28] Vatsal, V.H., Jha, B.K. and Singh, T.P. Generalised neuronal calcium dynamics of membrane and ER in the polar dimension. *Cell Biochemistry and Biophysics*, (2024). [CrossRef]

[29] Jha, B.K., Vatsal, V.H. and Singh, T.P. Navigating the fractional calcium dynamics of Orai mechanism in polar dimensions. *Cell Biochemistry and Biophysics*, (2024). [CrossRef]

[30] Joshi, H. Mechanistic insights of COVID-19 dynamics by considering the influence of neurodegeneration and memory trace. *Physica Scripta*, 99(3), 035254, (2024). [CrossRef]

[31] Purohit, S.D., Baleanu, D. and Jangid, K. On the solutions for generalised multiorder fractional partial differential equations arising in physics. *Mathematical Methods in the Applied Sciences*, 46(7), 8139-8147, (2023). [CrossRef]

[32] Vaishali and Adlakha, N. Disturbances in system dynamics of Ca^{2+} and IP_3 perturbing insulin secretion in a pancreatic β-cell due to type-2 diabetes. *Journal of Bioenergetics and Biomembranes*, 55, 151–167, (2023). [CrossRef]

[33] Naik, P.A., Eskandari, Z. and Shahraki, H.E. Flip and generalized flip bifurcations of a two-dimensional discrete-time chemical model. *Mathematical Modelling and Numerical Simulation with Applications*, 1(2), 95-101, (2021). [CrossRef]

[34] Manhas, N. Mathematical model for IP_3 dependent calcium oscillations and mitochondrial associate membranes in non-excitable cells. *Mathematical Modelling and Numerical Simulation with Applications*, 4(3), 280–295, (2024). [CrossRef]

[35] Kumar, P. and Erturk, V.S. Dynamics of cholera disease by using two recent fractional numerical methods. *Mathematical Modelling and Numerical Simulation with Applications*, 1(2), 102-111, (2021). [CrossRef]

[36] Nakul, N., Mishra, V. and Adlakha, N. Finite volume simulation of calcium distribution in a cholangiocyte cell. *Mathematical Modelling and Numerical Simulation with Applications*, 3(1), 17-32, (2023). [CrossRef]

[37] Podlubny, I. *Fractional Differential Equations* (Vol. 198). Academic Press: New York, USA, (1999).

[38] Miller, K.S. and Ross, B. *An Introduction to The Fractional Calculus and Fractional Differential Equations*. John Willey & Sons: New York, (1993).

[39] Kilbas, A.A., Srivastava, H.M. and Trujillo, J.J. *Theory and Applications of Fractional Differential Equations* (Vol. 204). Elsevier: Amsterdam, (2006).

[40] Diethelm, K. *The Analysis of Fractional Differential Equations: An Application-Oriented Exposition using Differential Operators of Caputo Type*. Springer: Heidelberg, (2010).

[41] Mainardi, F. and Pagnini, G. The Wright functions as solutions of the time-fractional diffusion equation. *Applied Mathematics and Computation,* 141(1), 51-62, (2003). [CrossRef]

[42] Keener, J. and Sneyd, J. *Mathematical Physiology* (Vol. 8/1). Springer: New York, (2009).

[43] Prista von Bonhorst, F., Gall, D. and Dupont, G. Impact of β-amyloids induced disruption of Ca^{2+} homeostasis in a simple model of neuronal activity. *Cells,* 11(4), 615, (2022). [CrossRef]

[44] Zhang, H., Sun, S., Wu, L., Pchitskaya, E., Zakharova, O., Tacer, K.F. and Bezprozvanny, I. Store-operated calcium channel complex in postsynaptic spines: a new therapeutic target for Alzheimer's disease treatment. *Journal of Neuroscience,* 36(47), 11837-11850, (2016). [CrossRef]

[45] Gil, D., Guse, A.H. and Dupont, G. Three-dimensional model of sub-plasmalemmal Ca^{2+} microdomains evoked by the interplay between ORAI1 and InsP_3 receptors. *Frontiers in Immunology,* 12, 659790, (2021). [CrossRef]

[46] Sneyd, J., Tsaneva-Atanasova, K., Bruce, J.I.E., Straub, S.V., Giovannucci, D.R. and Yule, D.I. A model of calcium waves in pancreatic and parotid acinar cells. *Biophysical Journal,* 85(3), 1392–1405, (2003). [CrossRef]

[47] Marambaud, P., Dreses-Werringloer, U. and Vingtdeux, V. Calcium signaling in neurodegeneration. *Molecular Neurodegeneration,* 4, 20, (2009). [CrossRef]

[48] Yagami, T., Kohma, H. and Yamamoto, Y. L-type voltage-dependent calcium channels as therapeutic targets for neurodegenerative diseases. *Current Medicinal Chemistry,* 19(28), 4816-4827, (2012). [CrossRef]

[49] Bezprozvanny, I.B. Calcium signaling and neurodegeneration. *Acta Naturae,* 2(1), 72-80, (2010).

[50] Jha, B.K., Adlakha, N. and Mehta, M.N. Finite volume model to study the effect of ER flux on cytosolic calcium distribution in astrocytes. *Journal of Computing,* 3(11), 74-80, (2011).

Bulletin of Biomathematics (BBM)
(https://bulletinbiomath.org)

How to cite this article: Jha, B.K., Vatsal, V.H. & Singh, T.P. (2024). The effect of amyloid beta, membrane, and ER pathways on the fractional behavior of neuronal calcium. *Bulletin of Biomathematics,* 2(2), 198-217. https://doi.org/10.59292/bulletinbiomath.2024009